INDONESIAN JOURNAL ON GEOSCIENCE
Geological Agency
Ministry of Energy and Mineral Resources

Journal homepage: http://ijog.geologi.esdm.go.id
ISSN 2355-9314, e-ISSN 2355-9306

Geological Trap Controlling the Residence Time of Groundwater in Assessment of Exploitation Zone for Its Sustainable Resources Case Study: The Slope of Karang Mount, Banten Province, Indonesia

Johanes Hutabarat[1], Azwar Satrya Muhammad[2,3], Teuku Yan Waliana Muda Iskandarsyah[1], Yudhi Listiawan[1], M. Ridfan Trisnadiansyah[3], Putu Ayu Andhira[3], and Hendarmawan[1]

[1]Faculty of Geological Engineering, Universitas Padjadjaran
[2]PT Tirta Investama Danone Indonesia
[3]Post Graduate Study, Faculty of Geological Engineering, Universitas Padjadjaran

Corresponding author: j.hutabarat@unpad.ac.id
Manuscript received: September, 20, 2023; revised: October, 24, 2023;
approved: November, 8, 2023; available online: November, 27, 2023

Abstract - The southern slope of Mount Karang is covered by complex volcanic deposits with complicated texture and structure. The study on zone or location of water resources which would be exploited required a comprehensive hydrogeological approach. Through detailed geological mapping, spring sampling, and well drilling were carried out. Representative spring water samples were taken to be analyzed in the laboratory, and to obtain the data of physical groundwater, chemical groundwater, stable isotopes ^{18}O (oxygen-18), and deuterium contents, as well as the age of the groundwater. In general, the groundwater facies of the studied area showed Ca, Na, $KHCO_3$ with several sites indicating changes to $CaHCO_3$ during the dry and rainy seasons. The synthesis results of the stable isotope ^{18}O (oxygen-18) and deuterium contents, verified by the physical and chemical groundwater controlled by geological setting in the groundwater subbasins, show the anomaly of residence time as trapped by the normal fault in the middle of the studied area. The existing normal fault might control this anomaly of residence time of groundwater surrounding site JH1, JH9, and JH20. However, the distribution of three different water source zones occurred. All group of groundwater indicated a complex flowing with geological setting controlling the physical, chemical content, and the age of the groundwater. At last, sites JH4, JH5, and JH9 show that the zones are proper to be developed as sustainability groundwater resources.

Keywords: groundwater facies, stable isotope, groundwater flow, sustainable water

© IJOG - 2023

How to cite this article:
Hutabarat, J., Muhammad, A.S., Iskandarsyah, T.Y.W.M., Listiawan, Y., Trisnadiansyah, M.R., Andhira, P.A., and Hendarmawan, 2023. Geological Trap Controlling The Residence Time of Groundwater in Assessment of Exploitation Zone for Its Sustainable Resources Case Study: The Slope of Karang Mount, Banten Province, Indonesia *Indonesian Journal on Geoscience*, 10 (3), p.419-432. DOI: 10.17014/ ijog-.10.3.419-432

Introduction

Background

Water resource sustainability has become a global concern for all stakeholders: the government, business activists, and community. The Indonesia government, researchers along with NGO also concerned with the environment issue. They actively proclaime how important water resource conservation and the groundwater balance to maintain the sustainability of water resource for their need. Moreover, the rapid industry development causes water need proportion increases.

Various approaches were made to gain potential knowledge based on hydrogeological conditions and water resource dynamic patterns. A research was conducted around the northern slope of Mount Karang, Banten Province, Indonesia. This area is a water resource to support Serang City as the province capital, besides to fulfil various Indonesian national strategic industries (Figure 1).

Research interest in this area is shown by previous studies including Nishimura *et al.* (1986; 1992), Iwaco and Associate (1987), Santosa (1991), Rusmana *et al.* (1991), Endyana *et al.* (2011), and Harada *et al.* (2014) who are oriented to the geological framework. Syariman and Hendarmawan (2010) presented measurements of the hydrological elements of rainfall to evapotranspiration. Meanwhile, Alam *et al.* (2014a; 2014b; 2019) and Hartanto *et al.* (2019; 2021; 2022) reveal hot spring water for geothermal potential. The Serang City is located in the northeast of Mount Karang with developing industrial activities (see Figure 1). It highly depends on Rawa Danau water resources. The water supply from the northern slope of Mount Karang is the key to the

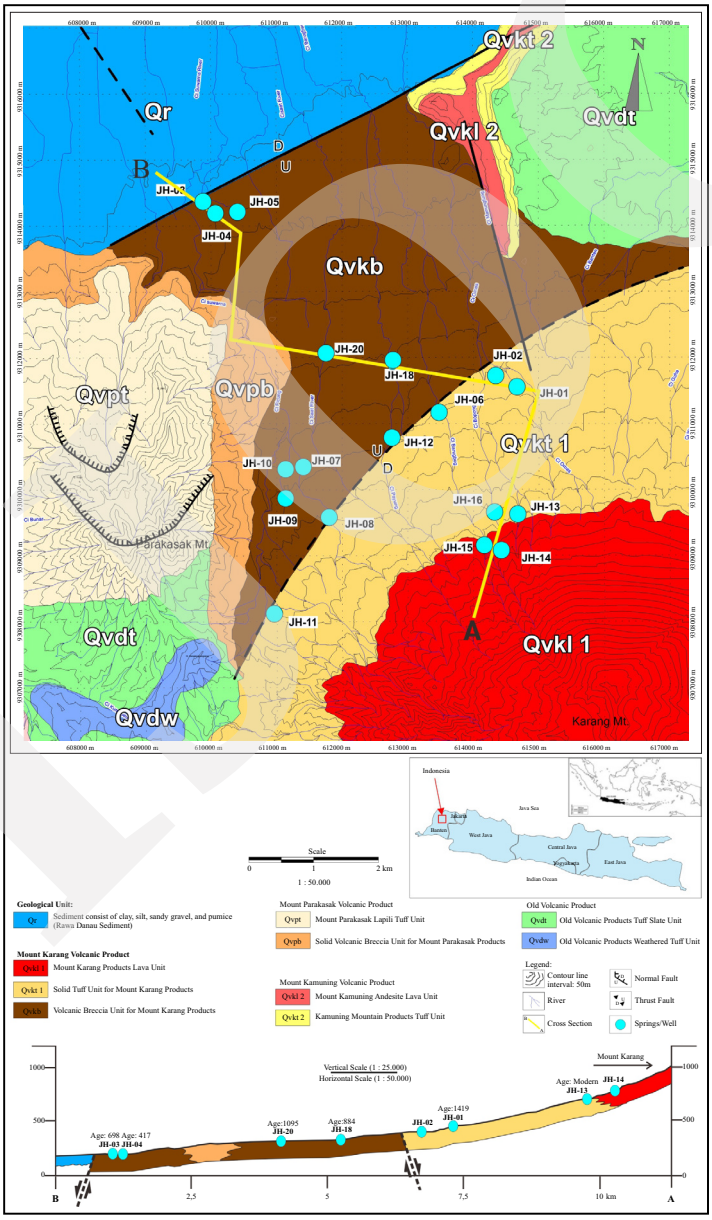


Figure 1. Geological setting of the studied area showing the distribution of sampling. (modified after Harada *et al.* 2014).

sustainability of water in Rawa Danau. However, database on the slope of Mount Karang is lack.

Disclosure of the groundwater characteristics related to the age or time of its existence in a certain zone, is often neglected in observations. Whereas determining water sources is very important to see its sustainability ((Putranto *et al*., 2020; Nugraha *et al*., 2021; Akurugu *et al*., 2022; Mahdid *et al*., 2022; Tyne *et al*., 2022; Chen *et al*., 2023). Research on water resources, especially in Indonesia, still depends on conventional hydrogeological (geological setting) approaches, very few use stable isotopes. However, the combination of these approaches will verify and validate each other (Singh, 2013; Alam *et al*., 2014; Kharisma *et al*., 2015; Bershaw and Lechler, 2019). The residence time of groundwater is related to the total travel distance and the average groundwater velocity as described by Darcy's Law. The groundwater moving through aquifer is equivalent to the basic content of the isotope dating during groundwater flowing from recharge to discharge (Loaiciga, 2004).

The geological setting, *i.e.* the lithology type, distribution, stratification, and architectural forms that differ from each other will become the water bearing formation. Water as the filling fluid moves following the geological setting of an area with its dynamics (García-Gil *et al*., 2023). The interaction of water and rocks along with the geological setting is indicated by the quality or the chemical content of the water (Suhendar *et al*., 2020; Gebeyehu *et al*., 2022). Meanwhile, groundwater is a dynamic substance that follows nature laws, and flows depends on the head of pressure and temperature as well as hydraulic gradients. However, both approaches will ultimately verify other analyses of the area condition (Rademacher *et al*., 2001; Thiébaud *et al*., 2010; Urrutia *et al*., 2019; Xia *et al*., 2022).

Serang City which is very strategic for Indonesia industries, highly requires support on the water resource supply. The Mount Karang area as the main water resources of Serang City has led a hydrogeology research in the direction of how groundwater storage conditions on the Mount Karang slopes for the sustainability of water supply. This paper shows empirical volcanic rock architecture with the fluid character of water when flowing in rocks as validated by the age or residence time of water.

Geographically, the studied area is located at -6°10' 39.4" to -6° 16' 33.8" E Latitude and 105°58' 6.7" to 106°3'37" Longitude (Figure 1). This research was carried out on November 2007 to December 2008, and analysis activities were carried out on January-July 2023 after obtaining validation from expertise in PT Tirta Investama - Danone, France.

Methods

Studying the geological conditions of the researched area through geological mapping approach by traversing an outcrop, was conducted in the field (Barnes and Lisle, 2004). This method used equipment including geological compasses, hammers, loupes, and topographical maps. Rock outcrops were observed in the field, and rock samples were determined to represent the researched area for mineral content analysis. The similarities and differences in rock types are mapped and presented in the form of geological maps. Groundwater sampling was carried out from springs and wells, and one from an exploration bore hole with the depth of 60 m below the surface.

The sampling method was carried out randomly and periodically from springs and wells. The contents of the isotope ^{18}O (oxygen-18) and isotope ^{2}H (deuterium) were identified using a mass spectrometer with prior preparation (Fritz and Fontes, 1981; IAEA-Vienna, 2009). Meanwhile, the age of the groundwater was determined especially after the subsurface geological features had been reconstructed.

^{18}O Isotope Analysis

Identification of the ^{18}O isotope content was carried out by reacting 2 ml of water sample with CO_2 gas, and shaking it for 4-6 hours until an isotope equilibrium was reached. From this reaction, the

^{18}O isotope was transferred from the water sample into CO_2 gas as the following equation:

$$H_2{}^{18}O + CO^{16}O \rightarrow H_2{}^{16}O + CO^{18}O \quad \text{..... (1)}$$

The CO_2 gas resulting from the reaction above, was then analyzed in the mass spectrometer to measure the $^{18}O/^{16}O$ ratio.

Deuterium Analysis

Deuterium identification was carried out through the reaction of water samples with Zn powder (shoot) at 450° C under vacuum conditions to produce H_2 gas as the equation below:

$$H_2O + Zn \rightarrow ZnO + H_2 \quad \text{..... (2)}$$

The H_2 gas produced from the above reaction, was then analyzed in the mass spectrometer to measure the D/H ratio.

Tritium Analysis (Age of Groundwater)

Tritium content identification in water sample was analyzed using electrolytic enrichment. Water samples were first distilled to remove minerals that might interfere in the counting process. About 3 gr of Na_2O_2 were added to 500 gr of distilled samples, then they were placed in steel electrolytic cells. After a week, about 20 gr of the water sample left in the cell was distilled again. As much as 10 ml of distilled-enriched samples were placed in counting vials with the addition of 10 ml of scintillation cocktail (Ultima Gold LLT). Counting was done using Liquid Scintillation Counter (LSC) Packard Tri-Carb in twelve cycles in 90 minutes/cycles for each sample. In addition, tritium standard spike before enrichment and spike after enrichment were also measured in the same batch of counting.

The physical properties of water such as pH, electric conductivity, temperature, and total dissolved solids were measured directly in the field with a portable equipment. Water chemical analysis was carried out at least from twenty springs and exploration wells, which were spread over various aquifers and elevations. All samples were tested by using ion chromatography metrohm for anions and cations, while the bicarbonate was tested using auto-titrator. The dominance of cations and anions is determined by Piper's (1944) trilinear diagram. Thus, the resulting groundwater facies could be used to verify the interpretation.

Result and Discussion

Geological Setting

The geological setting of the studied area located within West Java - Banten Block (Nishimura *et al*., 1986; 1992) comprises various rock formations, both Tertiary sedimentary rocks and mainly Quaternary volcanics with the succession as associated with Sunda Arc Quaternary volcanism in Java (Nishimura *et al*., 1992). The volcanic rock is known as Rawa Danau Complex as the centre for the pumice tuff eruption which is as "Tuff Banten" (Bemmelen, 1949), a product of Rawa Danau Volcanic Complex Caldera (Bemmelen, 1949; Kaars *et al*., 2001).

The volcanic activity in the Rawa Danau Complex started at Plio-Pleistocene, characterized by a succession of many volcanics, mainly andesite formed from several major volcanic bodies, active during successive phases, and culminating in a caldera formation period accompanied by an acid eruption (Bemmelen, 1949; Rusmana *et al*., 1991; Santosa, 1991).

The dominant geological structure in West Java-Banten Block area is northwest-southeast and northeast-southwest trends of fault which are the product of Early Miocene and Late Plio-Plistocene tectonic activities. There also found several lineages that have north-south and east-northwest-southwest and north-south trends (Bemmelen, 1949; Mulyadi, 1985; Santosa, 1991; Rusmana *et al*., 1991; Suryadarma and Fauzi, 1991). Several outcrops indicated displacement the Southern block relative to the Northern block of rock. These displacement form lineament along the fault, as shown in Figure 1.

Geological setting of the studied area were also identified based on the previous geologi-

cal information (Santosa, 1991; Rusmana *et al*., 1991; Endyana *et al*., 2011; Harada *et al*., 2014; Alam *et al.*, 2014a, 2014b, 2019), and further surveys carried out in this study. A prominent feature in the studied area is the presence of two volcanoes, namely Karang Volcano (1750 m msl.) located in the south part and Parakasak Volcano (793 m msl.) located in the south-southwest part of the researched area.

Geomorphologically, this area is dominated by volcanic landforms, with high terrain in the southwest-southern part and northeastern part, and low terrain in the northern part of 2 - 55^{o} slope. The terrains were composed of volcanic eruption products with a small portion of alluvial deposits. The highest elevation is 1,750 m asl. and the lowest elevation is 90 m asl.

The high terrain volcanic landform is steep, characterized by the morphology of the Karang Volcano and Parakasak Volcano, both of which are still in conical shape. Based on the distribution of concentric contours, the Karang Volcano shows that its northern part is steeper than the southern part, while the Parakasak Volcano shows its southern part is steeper than the northern one.

Geologically, of the studied area is mostly composed of pyroclastic deposits (tuff and volcanic breccias) and lava flows (dominantly andesite and minor basalt). The constituent lithological units can be divided into two main rock groups based on the products of caldera formation, namely pre-caldera and post-caldera.

The pre-caldera rock group comprises pyroclastic deposits, while the post-caldera rock group consists of pyroclastic deposits and lava flows. In addition, surface deposits in the form of alluvium are present as surface deposits. Figure 1 shows the geological setting of the studied area. In more detail, the pre-caldera consisting of rock group which is divided into two units, namely old volcanic products, from old to young, weathered tuff (Qvdw) and pumice tuff (Qvdt). Meanwhile, the post-caldera rock group is divided into seven units, *i.e*. Mount Kamuning volcanics from old to young consisting of tuff (Qvkt 2) and andesitic-basaltic lava flows (Qvkl 2); Mount Parakasak volcanics from old to young, comprising of volcanic breccia (Qvpb) and lapilli tuff (Qvpt); and volcanic products of Mount Karang, from old to young composed of volcanic breccias (Qvkb), tuffs (Qvkt 1), and andesitic-basaltic lava flows (Qvkl 1). In each rock unit, sedimentary stratigraphic relationships were observed in outcrops, and petrographic analysis was made on various volcanic products. The following is the geological succession of the area:

Old Volcanic Product Weathered Tuff Unit (Qvdw)

Qvdw is characterized by exposed rocks showing a very strong weathering level, composed of red-brown and reddish-grey tuff in a fresh condition. These deposits are part of the Rawa Danau Volcanic Complex, interpreted to be the oldest volcanic products.

Old Volcanic Product Tuff Slate Unit (Qvdt)

The Qvdt sediment is light grey-white to dark grey-brownish red, massive, fine- to coarse grained, is soft to moderate, clast supported, moderately disaggregated, and contains a significant fraction of the clast rounded white pumice, vesicular with a diameter of 1-5 cm. Petrographically it is vitric tuff with mineral assemblages composed of (in descending order of abundance) volcanic glass (+ pumice), plagioclase, rock fragments, pyroxene, opaque minerals, quartz, amphibole, iron oxide, chlorite, and clay minerals. This deposit was identified as part of the Banten Tuff.

Kamuning Mountain Product Tuff Unit (Qvkt 2)

Qvkt 2 is predominantly composed of light grey to dark grey tuff, fine- to medium grained with clastic material consisting of ash and lapilli with a small fraction of fine ash; matrix supported, moderately disaggregated, and very poor in coarse-grained materials.

Mount Kamuning Andesite Lava Unit (Qvkl 2)

Qvkl 2 is composed of andesite-basaltic lava flows, dark grey, dense, massive, moderately

vesicular, and some with sheeting joint at the bottom. The petrographic analysis shows a mineral assemblage comprising of plagioclase, pyroxene, opaque minerals, and iron oxide.

Solid Volcanic Breccia Unit for Mount Parakasak Products (Qvpb)

Qvpb is made up of volcanic matrix supported to clast support breccia, brownish colour, very poorly segregated, generally very solid, up to 1.5 m thick, composed of andesite-basaltic angular fragments, grey to reddish colour, up to 12 cm in size in a fine granular matrix, yellowish brown tuff, partially oxidized and weathered.

Mount Parakasak Lapilli Tuff Unit (Qvpt)

The Qvpt deposits are brownish to to yellowish grey colour, massive, matrix to clast supported, moderately to poorly disaggregated, and contain a significant fraction of white rounded pumice clast, medium vesicular up to 4 cm in diameter; mixed with the andesite-basaltic clast, angularly dense, brownish red, in small volumes. Petrographically, it lithic tuff with mineral assemblages composed of (in descending order of abundance) rock fragments, volcanic glass, clay minerals, chlorite, opaque minerals, quartz, and iron oxide.

Volcanic Breccia Unit of Mount Karang Products (Qvkb)

Qvkb is composed of volcanic matrix supported breccia, brownish to yellowish grey, poorly sorted, up to 1 m thick, comprising of andesite-basaltic angular fragments, gravel to boulder size, embedded in a matrix of tuff volcanic material. The results of petrographic analysis of rock fragments and matrix of mineral assemblages are composed of volcanic glass, rock fragments, plagioclase, pyroxene, quartz, and clay minerals.

Solid Tuff Unit of Mount Karang Products (Qvkt 1)

Qvkt 1 is predominantly composed of brownish yellow to reddish-brown tuff, fine-grained and solid, comprises of andesitic-basaltic crystals and lithic fragments, sometimes showing continuous and some discontinuous layers. Locally, dark brown to yellowish andesite lava flows, massive, about 35 cm thick occur.

Mount Karang Lava Product Unit (Qvkl 1)

The main type of Mount Karang lava products are andesitic to basaltic. The lava flows are dark grey, porphyric, vesicular, usually massive, and thick (5 m), joint sheet-like structures in several locations. Petrographically, mineral compositions are plagioclase, pyroxene, opaque minerals, and volcanic glass.

Geological Structure

Several faults could be identified as step slopes in the studied area have northeast-southwest trend. The structure could well be observed in the volcanic breccia (Qvkb) and lava (Qvkl 1) units of the Karang Volcano products. A normal fault in the middle of the studied area is possible to be the barrier for groundwater flowing from the upstream to downstream. Besides that, due to the fault becomes a secondary porosity, the groundwater flow system may have deep circulation along the fault. How far the relationship between groundwater and fault, can be verified by groundwater chemistry and stable isotope content (Jaunat *et al.* 2013; Galli *et al*. 2017).

Groundwater Chemistry

The groundwater physical characteristics that have been measured in the field are temperature, electrical conductivity (EC), total dissolved solids (TDS), spring discharges, and well discharges. The values obtained ranged from 20 - 26.2 ºC for water temperature and 22.7 - 31°C for air temperature, EC between 34 - 163 µS/Cm, TDS between 23 - 109 mg/l, and the flow rate around < 5 l/sec up to >100 l/sec. Meanwhile, the groundwater chemical properties was obtained from water quality analysis in the laboratory taken during the rainy season (March-April 2008) and during the dry season (August-October 2008). The results of field measurements and laboratory tests are presented in Tables 1, 2, and 3.

Groundwater Facies

The occurrence of springs and their chemical characteristics of groundwater is largely determined by the geological setting of the aquifer. Through geological outcrop data, the studied area is covered by the relatively impermeable and per-

Table 1. Data of Physical Properties of Groundwater and Springs in the Studied Area

No	Sample ID	Research Object	Lithology	Longitude (E)	Latitude	Elevation (masl)	pH	EC (µS/Cm)	TDS (mg/L)	Air Temp (°C)	Water Temp (°C)	Discharge (L/sec)
1	JH - 1	Spring	Breccia, Tuff	106,036	-6,227	320	7,2	89	59	26,9	25	10
2	JH - 2	Spring	Lava	106,033	-6,226	300	7,8	123	83	30,2	23,7	> 100
3	JH - 3	Well	Breccia	105,993	-6,202	131	6,8	163	109	29,3	26,3	-
4	JH - 4	Spring	Breccia	105,995	-6,204	145	6,8	125	84	27	25,5	>100
5	JH - 5	Spring	Breccia, Tuff	105,998	-6,203	160	6,2	128	86	26,6	25,3	>100
6	JH - 6	Spring	Lava	106,026	-6,231	350	6,9	128	85	26,1	23	10
7	JH - 7	Spring	Andesitic Lava	106,007	-6,238	320	6,4	111	75	26,2	24,7	50
8	JH - 8	Spring	Vesicular Lava	106,011	-6,245	370	6,7	133	89	25	23,8	>100
9	JH - 9	Spring	Tuff Breccias	106,005	-6,243	350	6,7	128	86	26,1	24,9	<10
10	JH - 10	Spring	Lava	106,005	-6,239	320	6,6	128	85	26	24,6	50
11	JH - 11	Spring	Lapilli Tuff	106,003	-6,258	430	6,7	91	61	26,2	24,8	20
12	JH - 12	Spring	Lava	106,019	-6,234	350	6,7	109	73	26,7	25,2	<10
13	JH - 13	Spring	Lava	106,037	-6,245	550	7,8	86	59	25	23,8	<5
14	JH - 14	Spring	Lava	106,034	-6,250	650	7,9	97	65	22,4	23,1	<5
15	JH - 15	Spring	Lava	106,032	-6,249	610	7,6	55	37	23,3	21,6	<5
16	JH - 16	Spring	Laharic	106,033	-6,244	550	7,1	29	20	23,4	22,9	<5
17	JH - 18	Spring	Unknown	106,019	-6,224	260	6,7	118	80	27,2	25	<5
18	JH - 20	Spring	Volcanic Breccias	106,010	-6,223	230	6,7	85	59	27,2	26,2	<10

Table 2. Data of Chemical Properties of Groundwater Sample During Dry and Rainy Seasons

No	Sample ID	Season	Cl^- (mg/L)	Na^+ (mg/L)	SO_4^{2-} (mg/L)	HCO_3^- (mg/L)	K^+ (mg/L)	Ca^{2+} (mg/L)	Mg^{2+} (mg/L)	Groundwater Facies
1	JH- 1	Dry	6,24	9,16	0,90	62,38	3,94	9,16	3,66	Ca, Na-K: HCO_3
		Rainy	4,42	7,90	0,69	56,01	3,10	8,22	1,99	Ca, Na-K: HCO_3
2	JH- 2	Dry	4,80	8,92	2,44	64,98	3,62	10,12	4,46	Ca, Na-K: HCO_3
		Rainy	4,90	8,12	4,03	67,22	3,63	12,33	1,99	Ca, Na-K: HCO_3
3	JH- 3	Dry	5,76	11,75	14,76	88,38	4,13	14,00	5,32	Ca, Na-K: HCO_3
		Rainy	3,92	11,29	6,16	87,13	4,08	15,62	4,24	Ca, Na-K: HCO_3
4	JH- 4	Dry	4,80	8,67	6,16	72,78	3,50	11,67	4,44	Ca, Na-K: HCO_3
		Rainy	4,42	8,65	4,96	64,73	3,10	13,15	3,49	Ca, Na-K: HCO_3
5	JH- 5	Dry	5,28	9,84	13,01	75,38	3,56	12,84	4,36	Ca, Na-K: HCO_3
		Rainy	3,91	8,12	4,96	64,73	3,59	13,15	3,74	Ca, Na-K: HCO_3
6	JH- 6	Dry	4,80	7,37	3,57	64,98	3,65	11,28	2,37	Ca, Na-K: HCO_3
		Rainy	3,43	6,85	2,22	74,68	4,00	13,97	3,98	Ca, Na-K: HCO_3
7	JH- 7	Dry	5,76	7,25	9,72	59,78	2,42	11,67	3,06	Ca, Na-K: HCO_3
		Rainy	5,89	6,05	8,93	47,30	2,19	11,50	3,98	Ca, Na-K: HCO_3
8	JH- 8	Dry	3,84	10,53	10,52	70,18	2,40	13,23	3,19	Ca, Na-K: HCO_3
		Rainy	5,39	7,19	11,60	58,50	2,69	14,79	4,48	Ca, Na-K: HCO_3
9	JH- 9	Dry	7,68	9,09	4,96	62,38	2,30	12,45	4,60	Ca, Na-K: HCO_3
		Rainy	4,42	7,44	5,20	69,71	2,22	14,79	4,24	Ca, Na-K: HCO_3
10	JH- 10	Dry	4,80	8,95	7,65	59,78	2,54	14,79	2,25	Ca: HCO_3
		Rainy	4,43	7,25	7,40	64,73	2,62	13,97	4,49	Ca, Na-K: HCO_3
11	JH- 11	Dry	7,68	7,37	5,92	38,99	0,83	8,56	3,22	Ca, Na-K: HCO_3
		Rainy	4,90	6,40	5,44	44,81	0,82	9,04	3,99	Ca, Na-K: HCO_3
12	JH- 12	Dry	5,76	9,09	1,12	64,98	1,90	13,23	3,19	Ca, Na-K: HCO_3
		Rainy	5,39	6,05	0,69	62,24	2,01	13,15	3,49	Ca: HCO_3
13	JH- 13	Dry	4,80	9,72	0,50	64,98	2,59	11,67	3,20	Ca, Na-K: HCO_3
		Rainy	3,43	6,57	3,11	59,75	2,27	10,69	2,99	Ca, Na-K: HCO_3
14	JH- 14	Dry	4,80	9,79	0,50	62,38	2,68	11,28	2,04	Ca, Na-K: HCO_3
		Rainy	3,92	7,50	0,69	62,24	2,30	12,33	1,99	Ca: HCO_3
15	JH- 15	Dry	4,80	6,15	0,90	36,39	2,44	7,00	1,82	Ca, Na-K: HCO_3
		Rainy	4,90	4,92	0,69	39,83	2,44	8,22	1,99	Ca, Na-K: HCO_3
16	JH- 16	Dry	4,32	9,84	2,89	57,19	1,72	6,23	2,77	Ca, Na-K: HCO_3
		Rainy	5,39	5,83	3,11	27,38	1,51	4,52	1,24	Ca, Na-K: HCO_3
17	JH- 17	Dry	7,68	10,20	7,15	57,19	3,20	13,23	4,12	Ca, Na-K: HCO_3
		Rainy	6,38	8,12	5,92	69,71	3,35	13,15	4,98	Ca, Na-K: HCO_3
18	JH- 18	Dry	6,24	9,65	6,17	51,99	2,42	10,89	2,74	Ca, Na-K: HCO_3
		Rainy	8,83	7,25	8,16	47,30	2,22	10,68	3,24	Ca, Na-K: HCO_3

Table 3. Data of Stable Isotope Content of Groundwater Sample During Dry and Rainy Seasons

No	Sample ID	Sampling I (Rainy)		Sampling II (Dry)		Sampling III (Transition)		Rainy Season				Dry Season			
		$\delta^{18}O$	δD	$\delta^{18}O$	δD	$\delta^{18}O$	δD	Tritium (TU)	^{13}C ($^{o}/_{oo}$)	pMC	Age (Year BP)	Tritium (TU)	^{13}C ($^{o}/_{oo}$)	pMC	Age (Year BP)
1	JH- 1	-7,8	-48,4	-8	-50,3	-7,9	-48,8	1,82	-13,04	78,40	1545	1,45	-13,50	79,60	1419
2	JH- 3	-6,5	-40,6	-6,7	-40,8	-6,6	-40,9	2,65	-13,71	89,43	456	2,18	-13,50	89,85	417
3	JH - 4	-6,3	-40,3	-6,4	-39	-6,5	-40,4	3,86	-13,75	96,56	Modern	2,12	-13,75	86,85	698
4	JH - 5	-6,2	-39,5	-6,4	-40,1	-6,4	-39,7	n.d.	n.d.	n.d.	n.d.	n.d.	n.d.	n.d.	n.d.
5	JH - 9	-8,7	-53,2	-6	-33,5	-7,3	-42,2	3,88	-14,2	100,64	Modern	n.d.	n.d.	n.d.	n.d.
6	JH - 13	n.d.	n.d.	-7,5	-46,5	-7,7	-46,8	n.d.	n.d.	n.d.	n.d.	n.d.	n.d.	n.d.	n.d.
7	JH- 15	-7,5	-45,3	-7	-44,9	-7,2	-44,9	3,98	-14,5	105	Modern	n.d.	n.d.	n.d.	n.d.
8	JH - 18	-6,7	-38,2	-6,4	-38,4	-6,6	-37,9	2,53	-14,2	87,27	658	1,87	-14	84,91	884
9	JH - 20	-7,6	-46,5	-7,5	-46,2	-7,5	-47	3,96	-14,5	108,2	Modern	1,69	-13,75	82,77	1095

meable rocks. Therefore, the groundwater subbasin distribution can be described. The determination of groundwater basins is in line with some researches on groundwater basins by Nisi *et al*. (2015), Daranond *et al*. (2020), Li *et al*. (2021), Toth *et al*. (2022), Akurugu *et al*. (2022), and Al Haj *et al*. (2023). The results of delineation of permeable and impermeable rocks are shown in Figure 2 as the distribution of groundwater subbasin.

Groundwater facies analysis and showed the contents of Ca, Na, $KHCO_3$, and $CaHCO_3$, indicating the presence of water-rock interaction during their flowing in the shallow or deep circulation aquifers (Figures 3 and 4) as described by Patel *et al*. (2023). In general, the groundwater facies are Ca, Na, $KHCO_3$ facies. The anomaly cases occurred in the development of $CaHCO_3$ in the site JH10 in the dry season, and sites JH12 and JH14 in the rainy season, respectively.

Stable Isotopes of Groundwater

Data on oxygen and deuterium isotope content from springs and wells are plotted in graphs to meet the global meteoric water line, as shown in

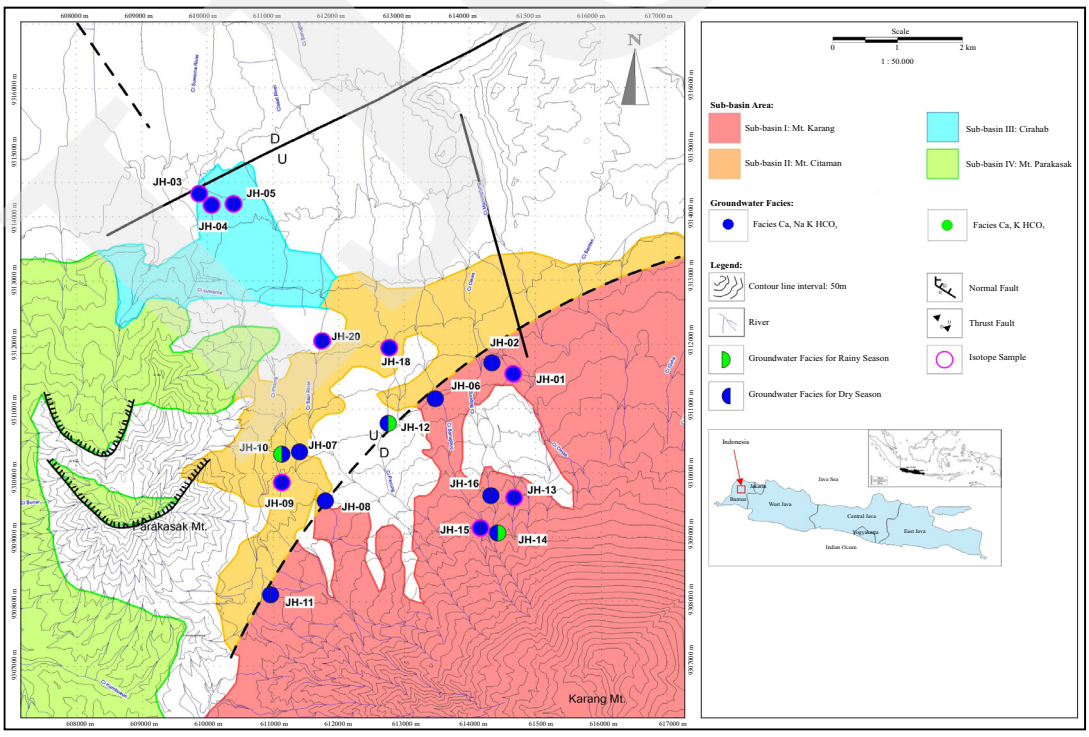


Figure 2. Distribution of groundwater subbasin and groundwater facies during the rainy and dry seasons.

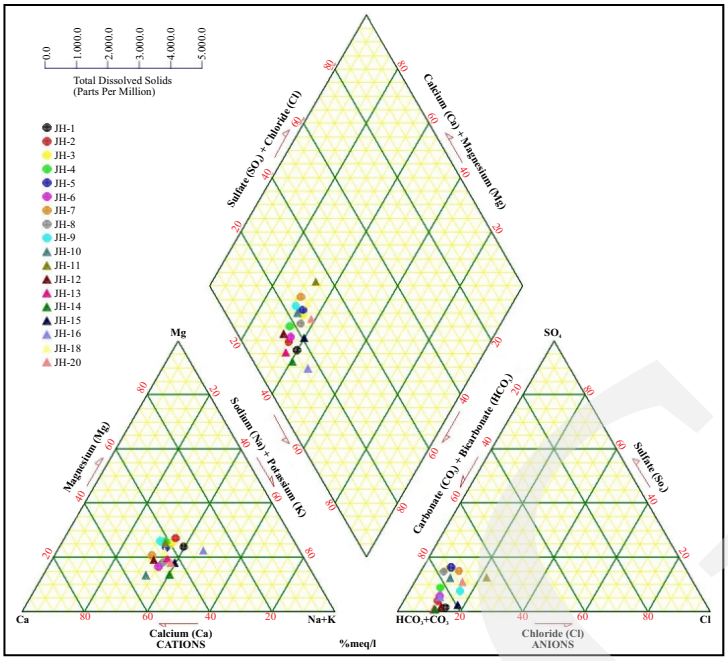


Figure 3. Trend of groundwater facies on the sites in the dry season.

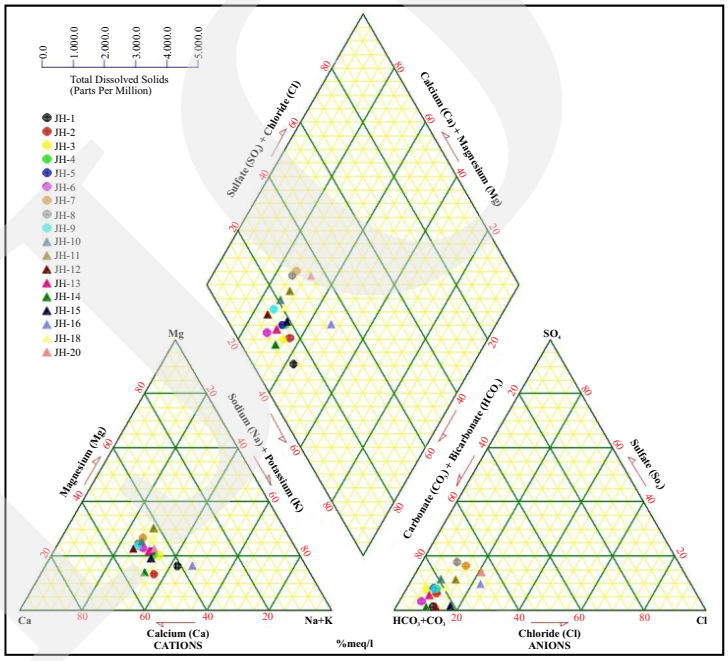


Figure 4. Trend of groundwater facies on the sites in the rainy season.

Figure 5. The groundwater trend of the oxygen and deuterium content on the studied area is close to the global meteoric water line. However, the very close trend might indicate that the studied area at that time (500 years to 1,100 years BP based on the groundwater age data on the studied area) was hotter compared to global conditions (Kolodny *et al*., 2009; Luz and Barkan, 2010; Hughes and Crawford, 2012; Kato *et al*., 2021; and Aron *et al*., 2021).

Based on the stable isotope content of oxygen and deuterium in groundwater, the studied area can be divided into three large groups. Group 1 consists of ^{18}O (oxygen-18) -6.7‰ and below, as

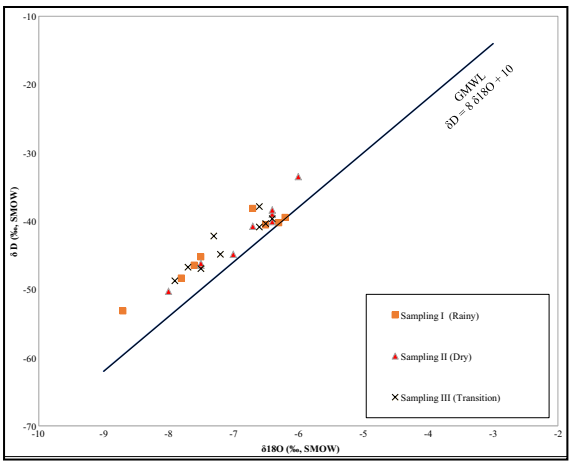


Figure 5. Trend of stable isotope content which is close to the global meteoric water line (Craig, 1961).

shown in site JH1, JH13, JH15, and JH20. Group 2 shows the content of ^{18}O (oxygen-18) -6.6 ‰ to ^{18}O (oxygen-18) -6.4 ‰, as shown in the site JH3 and JH18. Meanwhile, group 3 is represented by site JH4, JH5, and JH9 with a content of ^{18}O (oxygen-18) -6.3‰. This grouping provides a diversity indication of groundwater recharge places in various altitude areas of the catchment area. Meanwhile, plotting between ^{13}C and ^{18}O reveals that sites JH1, JH9, and JH20 might indicate an anomaly of residence time (Figure 6). The occurrence of these sites is controlled by geological setting on the basis of groundwater subbasin developing near the fault, indicating the groundwater flow in deep circulation. Such sites (JH1 and JH20) might be the recharge places on a short distance, but the residence time is longer. Meanwhile, for other groups, the stable isotope content has a quite linear trend.

Discussion

The geological conditions greatly determine the characteristic verification of the physical and chemical content of groundwater, as well as the content of stable isotopes of ^{18}O and deuterium, and the age of groundwater developing residence time in the studied area. However, the groundwater with rich Ca and HCO_3 content along with low EC (below 100 µS/Cm) may indicate the groundwater flow occurs at the top part (Freeze and Cherry, 1979; Clark and Fritz, 1997). Therefore, the interaction of groundwater and rocks rich in K-felsdspar (albit/Na+K >>) reflects a relatively long and deep circulation of groundwater flow with an EC value of more than 150 µS/cm. In general, groundwater facies type Ca, Na, $KHCO_3$ might indicate the spring and drilled well (the site JH3) flowing in an intermediate flow path. However, changes in sites JH10, JH12, and JH14 are greatly affected by the short groundwater flow. Their chemical

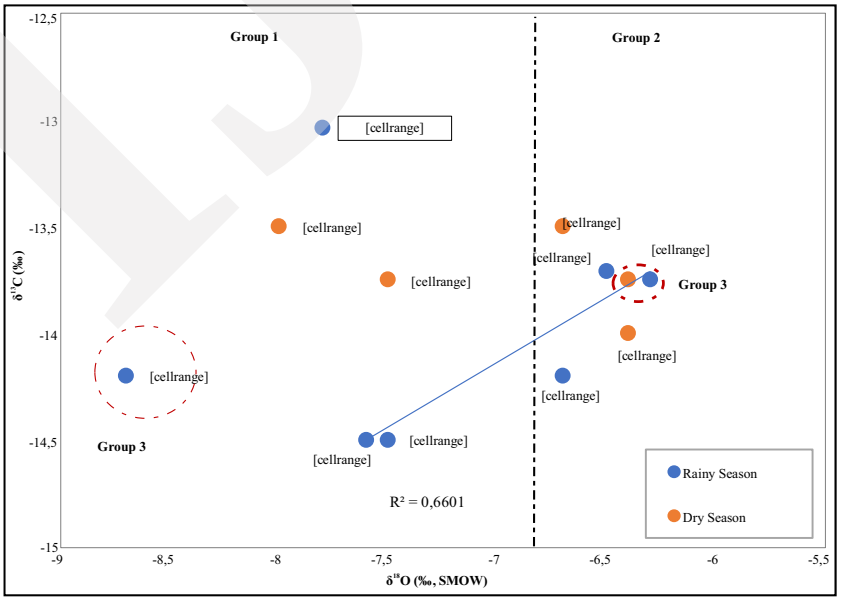


Figure 6. Anomaly of groundwater residence time in several sites.

contents indicated $CaHCO_3$ facies with an EC value is less than 100 µS/Cm.

The groundwater flow which is quite near to the catchment area is depicted in site JH1, JH13, JH15, and JH20. The interpretation of the flow nearest to the recharge place is supported by EC data, which is quite minor, and shown by the trend in the stable ^{18}O isotope content of group 1 (as shown in Figure 6). The formation of groundwater in these springs is easily to understand, because its existence is near the faults and related to subsurface groundwater basin boundaries. The movement of groundwater tends to circulate deeply and is detained. Hence, the water does not flow to the surface promptly and retained in the aquifer, and is certainly older than the other springs. The fault could be as a geological trap causing the residence time of groundwater long. The course of deep circulating water is verified by groundwater chemical facies type Ca, Na, $KHCO_3$ as described by Chebotarev (1955).

Some long to intermediate distance water movements are indicated by sites JH3 and JH18 in the studied area. Both water samples contain stable isotopes of group 2 ^{18}O. The chemical facies characteristic indicates rather intermediate or distance flow part, although it appears after the basin boundary, but is located near the fault. In contrast to the previous two types, sites JH4, JH5, and JH9 show indications of long-distance flow movement, and are supported by verification of EC data and chemical facies. Moreover, the presence of springs in groundwater subbasins does not move significant hindrance. The spring water tends to acquire a large discharge, and is intermediate in the age.

Based on groundwater characteristics and geological control, the water resources that are very sufficient for monitoring are sites JH4, JH5, and JH9. Groundwater flow system through those sites in the groundwater sub-basin might indicated that groundwater does not being obstructed during flow path. Thus, these locations are proper to be developed to meet the needs of industry in the southern part of Rawa Danau. However, a proper extraction needs to be calculated in more detail, and the catchment area is necessarily conserved.

Conclusion

The geological setting of the studied area divided into groundwater subbasins greatly controls the chemical characteristic and the stable isotope content of groundwater. However, such groundwater subbasins are not the barrier for groundwater flow system and might have been connected to each other. The geological trap controlling residence time of groundwater happened at sites JH1 and JH20, indicating older groundwater than other In general, springs in the studied area show groundwater flows that circulate deeply and moves short, intermediate, and long distance. Three sites were selected to be utilized to meet the needs of industrial areas in the southern part of Rawa Danau (Serang Regency), *i.e.* sites JH4, JH5 and JH9, due to their long-distance flow movement which are verified by EC data and chemical facies. This groundwater flow system indicates that the sustainability of groundwater resources is better than short distance or intermediate flow systems, needed by the industry.

Acknowledgment

The authors would like to express their gratitude and highest appreciation to the Director and Staff of PT Tirta Investama-Danone for the data permit, so that the authors could finish their manuscript.

References

Akurugu, B.A., Obuobie, E., Yidana, S.M., Stisen, S., Seidenfaden, I.K., and Chegbeleh, L.P., 2022. Groundwater resources assessment in the Densu Basin: A review. *Journal of Hydrology: Regional Studies,* 40, p.101017.

Alam, B.Y.C.S, Itoi, R., Taguchi, S., and Yamashiro, R., 2014a. Spatial Variation in Groundwater Types in the Mt. Karang (West Java, Indonesia) Volcanic Aquifer System Based on Hydro-Chemical and Stable Isotope

(δD and $\delta^{18}O$) Analysis. *Modern Applied Science,* 8 (6), p.87.

Alam, B.Y.C.S, Itoi, R., Taguchi, S., and Yamashiro, R., 2014b. Hydrogeochemical characterization and the origin of hot springs in the Cidanau Geothermal field, West Java, Indonesia. *Proceedings, 39th Workshop on Geothermal Reservoir Engineering Stanford University, Stanford, California*, February 24-26, SGP-TR-202.

Alam, B.Y.C.S., Itoi, R., Taguchi, S., Saibi, H., and Yamashiro, R., 2019. Hydrogeochemical and isotope characterization of geothermal waters from the Cidanau geothermal field, West Java, Indonesia. *Geothermics,* 78, p.62-69.

Al Haj, R., Merheb, M., Halwani, J., and Ouddane, B., 2023. Hydrogeochemical characteristics of groundwater in the Mediterranean region: A meta-analysis. *Physics and Chemistry of the Earth, Parts A/B/C*, p.103351.

Aron, P.G., Levin, N.E., Beverly, E.J., Huth, T.E., Passey, B.H., Pelletier, E.M., Poulsen, C.J., Winkelstern, I.Z., and Yarian, D.A., 2021. Triple oxygen isotopes in the water cycle. *Chemical Geology,* 565, p.120026.

Barnes, J.W. and Lisle, R.J., 2004. *Basic geological mapping, 4th edition*. John Wiley & Sons.

Bershaw, J. and Lechler, A.R., 2019. The isotopic composition of meteoric water along altitudinal transects in the Tian Shan of Central Asia. *Chemical Geology,* 516, p.68-78.

Bemmelen, R.W., 1949. *The Geology of Indonesia, Vol. 1, lA, lB*. Government Printing Office, Den Haag, 732pp.

Chebotarev, I.I., 1955. Metamorphism of natural waters in the crust of weathering-1. *Geochimica et Cosmochimica Acta,* 8 (1-2), p.22-48.

Chen, J., Yan, B., Xu, T., and Xia, F., 2023. Hydrochemical evolution characteristics and mechanism of groundwater funnel areas under artificial governance in Hengshui City, North China. *Ecological Indicators,* 148, p.110059.

Clark, I. and Fritz, P., 1997. *Environmental Isotopes in Hydrogeology*, Lewis Publisher.

Craig, H., 1961. Isotopic variations in meteoric waters. *Science,* 133 (3465), p.1702-1703.

Daranond, K., Yeh, T.C.J., Hao, Y., Wen, J.C., and Wang, W., 2020. Identification of groundwater basin shape and boundary using hydraulic tomography. *Journal of Hydrology,* 588, p.125099.

Endyana, C., Hirnawan, F., Hendarmawan, and Mardiana, U., 2011. Pendugaan nilai tahanan jenis batuan sebagai upaya untuk mengetahui struktur geologi yang berkembang pada endapan volkanik di Kecamatan Padarincang, Provinsi Banten. *Bulletin Sumber Daya Geologi,* 6, p.23-31.

Freeze, R.A. and Cherry, J.A., 1979. *Groundwater*. Prentice-Hall, Englewood Cliffs, NJ, 604pp.

Fritz, P. and Fontes, C.H., 1981. *Handbook of Environmental Isotope Geochemistry*, Elsevier Scientific Publisher Co., *Vol. 1*.

Galli, M.G., Damons, M.E., Siwawa, S., Bocanegra, E.M., Nel, J.M., Mazvimavi, D., and Martínez, D.E., 2017. Stable isotope hydrology in fractured and detritic aquifers at both sides of the South Atlantic Ocean: Mar del Plata (Argentina) and the Rawsonville and Sandspruit River catchment areas (South Africa). *Journal of South American Earth Sciences,* 73, p.119-129.

García-Gil, A., Jimenez, J., Marazuela, M.Á., Baquedano, C., Martínez-León, J., Cruz-Pérez, N., Laspidou, C., and Santamarta, J.C., 2023. Effects of the 2021 La Palma volcanic eruption on groundwater resources (part I). *Hydraulic impacts. Groundwater for Sustainable Development,* 23, p.100989.

Gebeyehu, A., Ayenew, T., and Asrat, A., 2022. Hydrogeochemistry of the groundwater system of the transboundary basement and volcanic aquifers of the Bulal catchment, Southern Ethiopia. *Journal of African Earth Sciences,* 194, p.104622.

Harada, A., Itoi, R., and Alam, B.Y.C.S., 2014. Development of a numerical model for groundwater flow, heat transportation and hydrogen stable isotope in Cidanau geothermal area. *Proceedings of International Symposium on Earth Sciences and Technology (CINEST)* 4-5 December, p.149-154.

Hartanto, P., Alam, B.Y.C.S., Lubis, R.F., and Hendarmawan, H., 2021. The Origin and Quality of the Groundwater of The Rawadanau Basin in Serang Banten, Indonesia. *Rudarsko-geološko-naftni zbornik,* 36 (2), p.11-24.

Hartanto, P., Alam, B.Y.C.S., Lubis, R.F., Ismawan, I., Iskandarsyah, T.Y.W., Sendjaja, Y.A., and Hendarmawan, H., 2022. The application of hydrogeochemical and stable isotope data to decipher the origin and evolution of hot springs in The Rawadanau Basin, *Indonesia. Geothermics,* 105, p.102506.

Hartanto, P., Delinom, R.M., and Hendarmawan, H., 2019. Type and Quality of Water at the Peak of Dry Season Based on the Major Elements of Water Chemical at Rawa Danau Serang Regency. *RISET Indonesian Journal of Geology and Mining,* 29 (1), p.13-25.

Hughes, C.E. and Crawford, J., 2012. A new precipitation weighted method for determining the meteoric water line for hydrological applications demonstrated using Australian and global GNIP data. *Journal of Hydrology,* 464, p.344-351.

IAEA-Vienna. 2009. *Laser Spectroscopic Analysis of Liquid Water Samples for Stable Hydrogen and Oxygen Isotopes*.

Iwaco and Associates, 1987. *West Java Provincial Water Sources Master Plan For Water Supply, Kabupaten Serang, Jakarta*.

Jaunat, J., Celle-Jeanton, H., Huneau, F., Dupuy, A., and Le Coustumer, P., 2013. Characterisation of the input signal to aquifers in the French Basque Country: Emphasis on parameters influencing the chemical and isotopic composition of recharge waters. *Journal of Hydrology,* 496, p.57-70.

Kaars, S. van der, Dan Penny, D., Tibby, J., Fluin, J., Dam, R.A.C., and Suparan, P., 2001. Late Quaternary palaeoecology, palynology, and palaeolimnology of a tropical lowland swamp: Rawa Danau, West-Java, Indonesia. *Palaeogeography, Palaeoclimatology, Palaeoecology 171*, 185-212.

Kato, H., Amekawa, S., Hori, M., Shen, C.C., Kuwahara, Y., Senda, R., and Kano, A., 2021. Influences of temperature and the meteoric water $\delta_{18}O$ value on a stalagmite record in the last deglacial to middle Holocene period from southwestern Japan. *Quaternary Science Reviews,* 253, p.106746.

Kharisma, H.L., Wijatna, A.B., and Wilopo, W., 2015. Aplikasi Isotop Alam untuk Mengetahui Asal-Usul Air Umbul Cokro, Kecamatan Tulung, Kabupaten Klaten. *Forum Teknik,* 36 (1).

Kolodny, Y., Calvo, R., and Rosenfeld, D., 2009. "Too low" δ18O of paleo-meteoric, low latitude, water; do paleo-tropical cyclones explain it? *Palaeogeography, Palaeoclimatology, Palaeoecology,* 280 (3-4), p.387-395.

Li, W.P., Wang, L.F., Zhang, Y.L., Wu, L.J., Zeng, L.M., and Tuo, Z.S., 2021. Determining the groundwater basin and surface watershed boundary of Dalinuoer Lake in the middle of Inner Mongolian Plateau, China and its impacts on the ecological environment. *China Geology,* 4 (3), p.498-508.

Loáiciga, H.A., 2004. Residence time, groundwater age, and solute output in steady-state groundwater systems. *Advances in Water Resources,* 27 (7), p.681-688.

Luz, B. and Barkan, E., 2010. Variations of $^{17}O/^{16}O$ and $^{18}O/^{16}O$ in meteoric waters. *Geochimica et Cosmochimica Acta,* 74 (22), p.6276-6286.

Mahdid, S., Chabour, N., Debieche, T.H., Drouiche, A. and Pistre, S., 2022. Robustness of DRASTIC Method for Groundwater Vulnerability Case of Wadi Nil Aquifer in Jijel, NE Algeria. *Indonesian Journal on Geoscience*, 9 (2), p. 229-246. DOI: 10.17014/ijog.9.2.229-246

Mulyadi, 1985. The Geophysical Investigation of Banten Geothermal Area, West Java. *7th New Zealand Geothermal Workshop*, 201-206.

Nishimura, S., Harjono, H., Suparka, S., 1992. The Krakatau Islands: The Geotectonic Setting. *GeoJournal,* 28 (2), p.87-98.

Nishimura, S., Nishida, J., and Hehuwat, F., 1986. Neo-Tectonics of the Strait of Sunda, Indonesia. *Journal of Southeast Asian Earth Sciences,* 1 (2), p. 81-91.

Nisi, B., Buccianti, A., Raco, B., and Battaglini, R., 2015. Analysis of complex regional data-

bases and their support in the identification of background/baseline compositional facies in groundwater investigation: developments and application examples. *Journal of Geochemical Exploration,* 164, p.3-17.

Nugraha, G.U., ALAM, B.Y.C.S.S.S.,Nur, A.A., Pranantya, P.A., Handayani, L., Lubis, R.F. and Bakti, H., 2021. Vertical Electrical Sounding Exploration of Groundwater in Kertajati, Majalengka, West Java, Indonesia. *Indonesian Journal on Geoscience*, 8 (3), p. 359-369. DOI: 10.17014/ijog.8.3.359-369

Patel, A., Rai, S.P., Akpataku, K.V., Puthiyottil, N., Singh, A.K., Pant, N., Singh, R., Rai, P., and Noble, J., 2023. Hydrogeochemical characterization of groundwater in the shallow aquifer system of Middle Ganga Basin, India. *Groundwater for Sustainable Development,* 21, p.100934.

Piper, A.M., 1944. A graphic procedure in the geochemical interpretation of water-analyses. *Eos, Transactions American Geophysical Union,* 25 (6), p.914-928.

Putranto, T.T., Winarno, T. and Susanta, A.P.A., 2020. Risk Assessment of Groundwater Abstraction Vulnerability Using Spatial Analysis: Case Study at Salatiga Groundwater Basin, Indonesia. *Indonesian Journal on Geoscience,* 7 (2), p. 215-224. DOI: 10.17014/ijog.7.2.215-224

Rademacher, L.K., Clark, J.F., Hudson, G.B., Erman, D.C., and Erman, N.A., 2001. Chemical evolution of shallow groundwater as recorded by springs, Sagehen Basin; Nevada County, California. *Chemical Geology,* 179 (1-4), p.37-51.

Rusmana, E., Suwitodirdjo, K., and Suharsono, 1991. *Geological Map of Serang Quadrangle, Jawa Barat*, *scale 1:100.000*. Geological Research and Development Centre, Bandung.

Santosa S., 1991. *Geological Map of Anyer Quadrangle, Jawa Barat*, *scale 1:100.000* Geological Research and Development Centre, Bandung.

Singh, B.P., 2013. Isotopic composition of water in precipitation in a region or place. *Applied Radiation and Isotopes, 75,* p.22-25.

Suhendar, R., Hadian, M., Muljana, B. and Setiawan, T., 2020. Geochemical Evolution and Groundwater Flow System in Batujajar Groundwater Basin Area, West Java, Indonesia. *Indonesian Journal on Geoscience*, 7(1), p. 87-104. DOI: 10.17014/ijog.7.1.87-104

Suryadarma, Fauzi A., 1991. Hydrothermal alteration of the Garung, Banten geothermal area, West Java. *Proceedings, 13th New Zealand Geothermal Workshop*, 193-197.

Syariman, P. and Hendarmawan, H., 2010. Analisis Fenomena Kehilangan Air Sungai Cisuwarna. *Jurnal Teknik Hidraulik*, 1 (1), pp.57-68.

Thiébaud, E., Dzikowski, M., Gasquet, D., and Renac, C., 2010. Reconstruction of groundwater flows and chemical water evolution in an amagmatic hydrothermal system (La Léchère, French Alps). *Journal of Hydrology,* 381 (3-4), p.189-202.

Tóth, Á., Kovács, S., Kovács, J., and Mádl-Szőnyi, J., 2022. Springs regarded as hydraulic features and interpreted in the context of basin-scale groundwater flow. *Journal of Hydrology,* 610, p.127907.

Tyne, R.L., Barry, P.H., Cheng, A., Hillegonds, D.J., Kim, J.H., McIntosh, J.C., and Ballentine, C.J., 2022. Basin architecture controls on the chemical evolution and ^{4}He distribution of groundwater in the Paradox Basin. *Earth and Planetary Science Letters,* 589, p.117580.

Urrutia, J., Herrera, C., Custodio, E., Jódar, J., and Medina, A., 2019. Groundwater recharge and hydrodynamics of complex volcanic aquifers with a shallow saline lake: Laguna Tuyajto, Andean Cordillera of northern Chile. *Science of the Total Environment,* 697, p.134116.

Xia, Q., He, J., Li, B., He, B., Huang, J., Guo, M., and Luo, D., 2022. Hydrochemical evolution characteristics and genesis of groundwater under long-term infiltration (2007-2018) of reclaimed water in Chaobai River, Beijing. *Water Research,* 226, p.119222.